SCANNING FLUORESCENCE CORRELATION SPECTROSCOPY

I. Theory and Simulation of Aggregation Measurements

N. O. PETERSEN
Department of Chemistry, The University of Western Ontario, London, Ontario, Canada N6A 5B7

ABSTRACT Scanning Fluorescence Correlation Spectroscopy (S-FCS) is introduced as an adaptation of Fluorescence Correlation Spectroscopy (FCS) to measure aggregation in systems, such as biological cell membranes, where diffusion or flow is slow. The theoretical framework for interpretation of S-FCS measurements are discussed in this paper with emphasis on the limitations arising from the sample size and shape. Computer simulations of the experiment demonstrate the potential of the technique and illustrate how some of the limitations may be overcome.

INTRODUCTION

Diffusion of proteins in plasma membranes of animal cells in culture is restricted in two ways: one fraction moves freely but more slowly than expected and another moves too slowly to be detected in Fluorescence Photobleaching Recovery (FPR) measurements (1, 2, 3). The mechanism whereby protein diffusion is impeded or prevented is not fully understood, and may in fact depend on the particular cell surface protein and on the cell type (4, 5). It is possible that protein-protein aggregation contributes to this restricted diffusion.

Protein aggregation has been observed directly by electron microscopy (6, 7) and has been inferred from fluorescence energy transfer experiments (8, 9). Moreover, modern fluorescence microscopy techniques have provided indirect evidence for "micro-clustering" of membrane receptors upon binding of hormones, such as growth factors and insulin (10, 11). However, quantitative in vivo measurements of the extent or rate of aggregation have been difficult and the mechanisms of aggregation remains obscure.

In this report we introduce a new experimental approach to making quantitative measurements of the distribution of fluorescently labeled proteins on the surfaces of living cells in culture. The technique, which we call Scanning Fluorescence Correlation Spectroscopy (S-FCS) is based on the analysis of fluctuations in fluorescence intensity measured with a focused laser beam across the surface of appropriately labeled cells. S-FCS is a special case of Fluorescence Correlation Spectroscopy (FCS) for uniform flow (12) designed for systems where diffusion, or flow, is slow. The principle of S-FCS is similar to that used, in a rotating cell geometry, to measure the weight average molecular weight of DNA by fluctuation spectroscopy (13). Here we describe the S-FCS experiment as applied to measurements on cell surfaces and present the theoretical framework for estimating mean aggregate sizes. We also report on computer simulations of the S-FCS experiments that aid in the examination of the statistical limitations of the experiment, with particular emphasis on the special problems that arise when the fluctuation records are limited in length by the size of the cell. In an accompanying contribution (14) we report on the application of S-FCS to the study of virus glycoprotein aggregation during budding of a membrane-enveloped virus from the host cell.

THEORY

Concentration Correlation Spectroscopy (15) and Fluctuation Spectroscopy (16) describe a collection of techniques which differ principally in the manner in which the concentration, and hence fluctuations in concentration, is monitored. FCS (12, 17, 18) represents the special case where the concentration is measured by the fluorescence intensity such that

$$i(t) = \rho\epsilon Q \int I(\mathbf{r})\, C(\mathbf{r}, t)\, d^3\mathbf{r}, \qquad (1)$$

where ρ is an instrumental factor accounting for the efficiency of collecting and counting the emitted photons, ϵ is the extinction coefficient and Q the quantum yield of the fluorescence of the probe molecule, and $I(\underline{r})$ is the intensity of the exciting light at position $\underline{r}$. For $\bar{\bar{F}}$CS it has been shown (17) that the variance of the relative intensity fluctuation is inversely related to the mean number of molecules, $\bar{N}$, in the observation area. The variance can be measured as the zero-time value ($G(0)$) of the intensity autocorrelation function, i.e.

$$\frac{G(0)}{\bar{i}^2} = \frac{\langle(\delta i)^2\rangle}{\bar{i}^2} = \frac{1}{\bar{\bar{N}}}. \qquad (2)$$

Here the autocorrelation function is defined by $G(\tau) = \langle \delta i(t)\delta i(t+\tau)\rangle$, with $\delta i(t) = i(t) - \bar{i}$ and $\bar{i}$ denoting the average intensity. For a uniform flow at a velocity V perpendicular to the direction of illumination with a Gaussian laser beam (12)

$$G(\tau) = G(0)\exp(-(\tau \cdot V/w)^2), \tag{3}$$

where w is the radius of the laser beam when the intensity is e^{-2} of the central intensity.

In S-FCS experiments a flow velocity is imposed by translating the sample at a uniform, known velocity through a laser beam. Independently, the beam radius w is measured so that the only unknown parameter in $G(\tau)$ is the scaling factor, $G(0)$.

The autocorrelation function is particularly sensitive to strongly absorbing or fluorescing components in systems containing several fluorescent species. The normalized autocorrelation function $g(\tau) = G(\tau)/\bar{i}^2$ has a zero-time value given by (17)

$$g(0) = \frac{G(0)}{\bar{i}^2} = \frac{1}{V}\frac{\sum_j (\epsilon_j Q_j)^2 \bar{c}_j}{\left(\sum_j \epsilon_j Q_j \bar{c}_j\right)^2}, \tag{4}$$

where the subscript refers to the jth species, the sum is over all fluorescent species, V is the volume observed in the experiment and $\bar{c}_j$ is the mean concentration of the jth species. Eq. 4 may be applied to an aggregated system when the sum is taken over the distribution of aggregates. Assuming that the molar extinction coefficient (ϵ) and the quantum yield (Q) of the monomer are unaffected by the number (n) of monomers per aggregate, i.e., $\epsilon_n = n\epsilon$ and $Q_n = Q$, then one can show that

$$g(0) = \frac{1}{\bar{N}_m}\left(\frac{\sigma^2 + \mu^2}{\mu}\right). \tag{5}$$

Thus $g(0)$ depends on the mean (μ) and the variance (σ^2) of the distribution and on the mean number of monomers ($\bar{N}_m$) in the observation volume.

The mean intensity, is $\bar{i} = \frac{1}{2}\, a\, \bar{N}_m$, where $a = \rho I_0 \epsilon Q$ is a constant that depends only on instrumental factors, incident illumination intensity, and spectroscopic properties of the probe. The product

$$g(0) \cdot \bar{i} = \frac{1}{2}\, a\left(\frac{\sigma^2 + \mu^2}{\mu}\right) \tag{6}$$

depends only on the mean and variance of the distribution and not on the total monomer concentration.

If the distribution is multimodal, namely a simple sum of several unimodal distributions individually characterized by their mean number of aggregates ($\bar{N}_i$), their mean (μ_i) and their variance (σ_i), then

$$g(0) = \frac{1}{\bar{N}_m^2}\Sigma \bar{N}_i(\sigma_i^2 + \mu_i^2), \tag{7a}$$

since $\bar{N}_m = \Sigma_i \bar{N}_i\mu_i$. Similarly

$$g(0) \cdot \bar{i} = \frac{a}{2\bar{N}_m}\Sigma \bar{N}_i(\sigma_i^2 + \mu_i^2). \tag{7b}$$

Table I summarizes the results of Eq. 7 *a* and 7 *b* for three types of bimodal distributions: (*A*) when both modes are Poisson distributions for which the variance equals the mean; (*B*) when the aggregates with larger mean are Poisson distributed while those with smaller mean are sharply peaked (with negligible variance); and (*C*) when both distributions have negligible variances. Table I also contains the results corresponding to monomer ($\mu = 1$)-oligomer equilibria and the limits of unimodal distributions. The results are expressed in terms of the mole fraction of monomers in aggregates, defined by $\bar{x}_i = \bar{N}_i\mu_i/\bar{N}_m$, and the ratio of the distribution means, $n = \mu_2/\mu_1$. The simple aggregation reaction $n\mathrm{A} \rightarrow \mathrm{A}_n$ has been considered previously (17) with the result listed for case *C* when $\mu_1 = 1$. For large aggregates $g(0)$ measures the mean number of aggregates, $\bar{N}_a$, in the observation volume since $g(0) = \mu/\bar{N}_m = 1/\bar{N}_a$ and $g(0) \cdot \bar{i}$ measures the mean number of monomers per aggregate since $g(0) \cdot \bar{i} = \frac{1}{2}\, a\mu$. These relations form the basis for the simplest interpretation of the scanning fluorescence correlation spectroscopy measurements presented previously (3).

Fluorescence photobleaching measurements yield measurements of the rate and extent of fluorescence recovery. The rate of recovery is used to calculate a diffusion coefficient, D, while the extent of recovery is interpreted as the fraction X_m of molecules that are free to diffuse (19). It

TABLE I
THE FUNCTIONS $g(0)\cdot\bar{N}_m = 2g(0)\bar{i}/a$ FOR VARIOUS AGGREGATE DISTRIBUTIONS

Distribution	Bimodal		Unimodal
	$\mu_2 > \mu_1 > 1$	$\mu_2 > \mu_1 = 1$	(limit of $x_2 = 1$)
A: $\sigma_1^2 = \mu_1$ $\sigma_2^2 = \mu_2$	$1 + (1+(n-1)x_2)\mu_1$	$(2 + (n-1)x_2$	$(1 + \mu)$
B: $\sigma_1^2 \ll \mu_1^2$ $\sigma_2^2 = \mu_2$	$x_2 + (1+(n-1)x_2)\mu_1$	$(1 + nx_2)$	$(1 + \mu)$
C: $\sigma_1^2 \ll \mu_1^2$ $\sigma_2^2 \ll \mu_2^2$	$(1 + (n-1)x_2)\mu_1$	$(1 + (n-1)x_2)$	μ

is possible that the mobile molecules are monomers that are free to diffuse, and that the immobile molecules are restricted from diffusing because they are part of large aggregates of monomers. Then the cell surface receptors are in a bimodal distribution where X_m is the fraction of free monomers and $(1 - X_m)$ is the fraction of monomers in the large aggregates. Case B with $\mu_1 = 1, x_2 = (1 - X_m)$ and $n \gg 1$ yields $g(0) = (1 - X_m)n/\bar{N}_m$. Thus $g(0)$, measured by S-FCS, should vary linearly with the fraction of immobile receptors, $(1 - X_m)$, measured by FPR.

METHODS

S-FCS Experiment

The fluorescence intensity measurements are performed with the fluorescence microscope equipment designed for spot-photobleaching measurements described previously (19, 20).

The sample is translated linearly and horizontally by a custom-designed translating stage driven by the output from a digital-to-analog converter, which in turn is controlled by a MINC-11/23 computer. The translating stage (built by W.M. McConnaughey, Washington University Medical School, St. Louis, MO) has a position detector which, through feedback circuitry, permits control of the sample position with a precision of ~20 nm. The translation is linear over a range of ~80 μm. The vertical displacement of the sample is <1% of the horizontal movement. The translating stage is moved in 1,024 discrete steps with a counting interval of 40–200 ms per step. During the period of a full range translation, there are no significant drifts. The sample is only exposed to the illumination of the laser beam during the active phase of the translation measurement.

Sample Preparation

The S-FCS measurements were performed on 3T3-cells cultured on glass coverslips in Dulbeccos Minimum Essential Medium with 10% Fetal Calf Serum and 1% Gentamycin. The cells were fixed in 3% paraformaldehyde in phosphate buffered saline for 15 min at room temperature, and then labeled with Fluorescein isothiocyanate derivatized wheat germ agglutinin (FITC-WGA; Sigma Chemical Co., St Louis, MO) or succinyl-concanavalin A (FITC-S-conA; Sigma Chemical Co.). After rinsing, the coverslips were inverted and mounted in 90% glycerol with 10% TRIS buffer at pH 8. The samples were observed with a 100X oil immersion objective (NA 1.35) and analyzed with a 0.75 μm radius laser beam at a wavelength of 488 nm.

Correlation Analysis and Fitting

The fluorescence data records are analyzed by a direct calculation of the autocorrelation function as

$$g(k \cdot \Delta x) = \frac{\frac{1}{N_k}\sum_{\ell=1}^{N_k} i(\ell \cdot \Delta x) i((\ell + k)\Delta x)}{\left(\frac{1}{N}\sum_{\ell=1}^{N} i(\ell \cdot \Delta x)\right)^2} - 1, \qquad (8)$$

where Δx is the step resolution, N the total record length, $N_k = N - k$. This estimate of the autocorrelation function is fit to a modified version of Eq. 3, namely

$$g(k\Delta x) = g(0) \exp(-(k\Delta x/w)^2) + g_0, \qquad (9)$$

using a least-squares fitting program with three variables: $g(0)$, w, and g_0.

Simulation Calculations

Simulation of S-FCS experiments are performed by numerical integration of random distributions of monomers or aggregates using convolution functions that simulate the laser intensity distribution and the collection efficiency of the optics. The spatial distribution of monomers and aggregates is determined by selecting x and y coordinates with a random number generator. Each point selected is assigned an integral number of monomers chosen randomly but constrained, such that the total monomer distribution represents a specified aggregation distribution. The distribution is restricted to a plane surface by letting the z-coordinate be a function of the x-coordinate. This permits simulation of a flat cell surface (z = constant) or a cell surface with contour (e.g., $z = a_0 + a_1x + a_2x^2 + a_3x^3 + a_4x^4$).

The simulated fluorescence intensity at a particular position is calculated as the sum of the concentration of monomers $c(\underline{r}, \ell \cdot \Delta x)$ within a radius of $2w$, multipled by the intensity $I(\underline{r})$ of the laser beam at the location of the aggregate and by the efficiency ($\epsilon(\underline{r})$), whereby the emission is collected and imaged on the photomultiplier (21, 22). This is the numerical integration of Eq. 1, with the optical parameters normalized such that the constant $a = \rho I_0 \epsilon Q$ is unity. The calculation is performed sequentially at a defined step resolution (Δx) over a total range of 50–80 μm in a thousand steps. The simulated intensity data are analyzed by Eq. 8 and the results fit to Eq. 9.

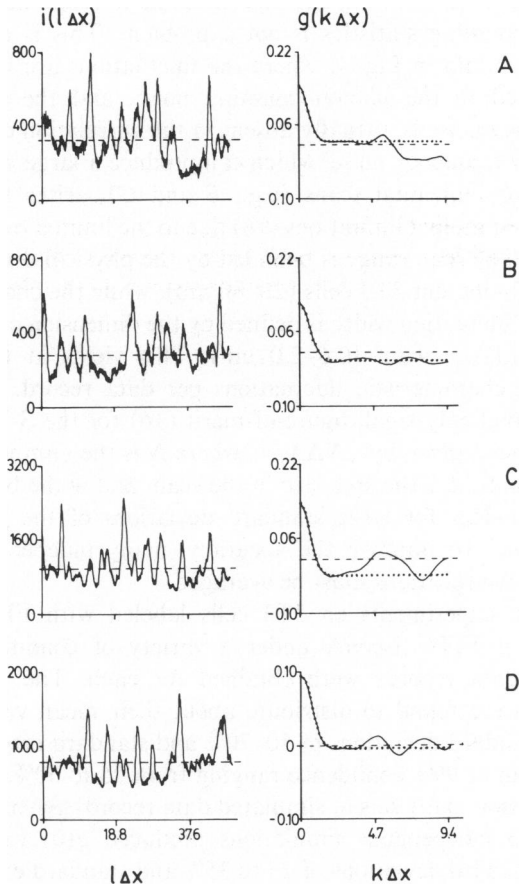

FIGURE 1 Examples of S-FCS data records and the corresponding correlation functions for 3T3 cells labeled with FITC-S-ConA (A and B) or FITC-WGA (C and D). The best fit to the correlation functions are shown with the dotted line, while the dashed lines correspond to $g(k\Delta x) = 0$ or $i(l\Delta x) = \bar{i}$. The fits yielded $g(0)$ values of 0.124 (A), 0.123 (B), 0.156 (C), and 0.098 (D). The l and k parameters correspond to the channel numbers in the digital records, Δx, the step resolution, is 47 nm and $l\Delta x$ and $k\Delta x$ are shown in units of micrometers.

RESULTS AND DISCUSSION

Fig. 1 shows four examples of fluorescence intensity data, $i(\ell\Delta x)$, for 3T3-cells labeled with FITC-S-conA (A, B) or FITC-WGA (C, D). The corresponding correlation functions, $g(k\Delta x)$, are also shown with the best fit (. . .) to the function in Eq. 9. The experimental correlation functions conform closely to Eq. 3 for the early portion of the data, but deviate significantly for large correlation distances (large k values in Eq. 9). Accordingly, only the first 30–50 data points are used for fitting and an empirical offset, g_0, is required. It is evident that the $g(0)$ value can be calculated with good precision from these data, but the magnitude of g_0 could seriously affect the accuracy of the S-FCS measurements.

Theoretical analysis (23) of the statistical accuracy of FCS measurements shows that the signal-to-noise ratio depends on the number of photoncounts per correlation time, per fluorescent molecule, and on the square root of the ratio of total experimental run time to the correlation time. For S-FCS experiments the count time per data point depends on the scan velocity and since one can scan slowly, photoncounting statistics is not a problem. This is clear from the data in Fig. 1, where the fluctuations are large compared to the photon counting noise, and the high frequency noise is virtually absent in the correlation data. The low frequency noise, which can produce a large value of g_0 for individual scans (e.g., B and C), arises from random sampling limitations (16) due to the limited record length. The scan range is bounded by the physical dimensions of adherent 3T3 cells (20–80 μm), while the characteristic fluctuation width is defined by the dimension of the focused laser beam (0.6–2.0 μm). This yields at most 40–100 characteristic fluctuations per data record. The correspondingly small figure-of-merit (16) for the S-FCS experiment, given by $\sqrt{N}\Delta X/w$, where N is the number of data points, ΔX the step size in the scan, and w the beam size, provides for large standard deviations of the $g(0)$ estimates. To improve the accuracy, many independent correlation functions must be averaged.

In 40 experiments on 3T3 cells labeled with FITC-WGA or FITC-S-conA under a variety of conditions, 20–25 data records were obtained for each. The $g(0)$ values were found to distribute about their mean values with standard deviations of 50–70% and standard error of the mean at 99% confidence ranging from 25 to 50%. For comparison many sets of simulated data records generated from 25 independent simulations produced $g(0)$ values with standard deviations of 25 to 35% and standard errors of the mean of 20% or less. The variations in experimentally determined $g(0)$ values are therefore larger than expected from statistical limitations of the data.

The effect of the number of data points used in the fitting is minimal. A set of 25 simulated data records were fit by the first 20, the first 30, or the first 40 data points. For individual data sets the $g(0)$ values varied by up to 10%, but the average estimate of $g(0)$ was insensitive to the number of data points used. The data analysis and fitting procedures do not, therefore, introduce additional inaccuracies.

Large aggregates with physical dimensions comparable to the beam dimension will distort the shape of the autocorrelation function and could give rise to errors in $g(0)$. However, for the 530 data sets analyzed, the beam radius estimated from the fits is 0.86 ± 0.1 μm, which agrees with that determined independently (0.75 μm) for the laser beam used here. The aggregate dimension, therefore, does not appear to be a problem.

Careful examination of data from several experiments suggests that the large variations in experimental $g(0)$ values arise from heterogeneity among the cells. The $g(0)$ values obtained from measurements on several regions on the same cell distribute with a standard error of the mean 1.5–3-fold smaller than that for the corresponding measurements on many cells in the same population. This cell-to-cell variation could reflect real differences in the receptor distributions, or could be a reflection of differences in cell shape or contour. For comparison experiments, we believe the best protocol is to sample a large number of cells to get an average $g(0)$ value for the conditions under investigation.

The contour of the cell will introduce three additional sources of intensity fluctuations: those arising from changes in surface area because the membrane has a curvature or is inclined relative to the beam; those arising from changes in the surface area as the membrane moves in and out of focus of the converging and diverging laser beam; and those arising from changes in the illumination intensity and detection efficiency at planes above and below the focal plane.

Fig. 2 A is a schematic representation of the contour of a typical adherent 3T3 fibroblasts as well as the divergence of the laser beam along the z-direction for a 1-μm beam (22). Figs. 2 B, C, and D show an approximation to the cell contour used in simulation experiments. The "fluorescent" particles were confined to a plane defined by $z = a_0 + a_2x_2^2 + a_4x_4^4$, with the values of the coefficients chosen to give a maximum "cell" thickness of 8 μm. Scans were performed at three levels of focus corresponding to $z = 0$ μm (Fig. 2 B) $z = 4$ μm (Fig. 2 C) and $z = 8$ μm (Fig. 2 D). Three examples of the simulated intensity scans are shown in Figs. 2 E, 2 F, and 2 G. In all three cases the fluctuation amplitudes are greatest when the cell membrane is in focus (at the edges in Figs. 2 B and 2 G, about halfway to the centre in Figs. 2 C and 2 F, and at the centre in Figs. 2 D and 2 E). Both the fluorescence level and the fluctuation amplitudes decrease when the membrane is out of focus. The hatched area in Figs. 2 B, 2 C, and 2 D indicate the effective detection volume for the optical geometry used in the simulation and corresponds to the volume within which the detected intensity exceeds e^{-4} times that at the centre of the beam at the focal plane.

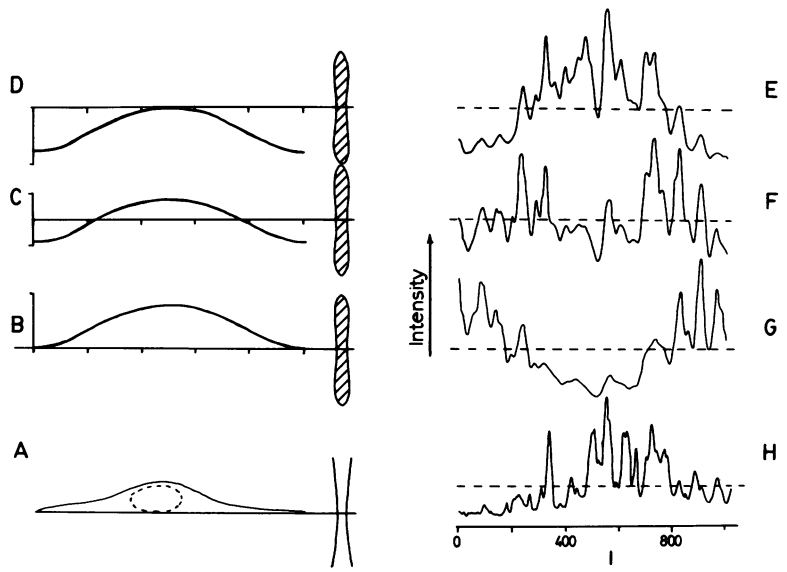

FIGURE 2 Illustrations of the effects of cell contour on real and simulated intensity scans. See text for details.

Fig. 2 *H* shows an experimental fluorescence intensity record on a 3T3 cell labeled with FITC-WGA corresponding to the scan at a focus at the top of the cell (compare Figs. 2 *E* and 2 *D*).

A series of simulations like those illustrated in Fig. 2 give $g(0)$ values of 0.109 (for $z = 0$ μm) 0.120 (for $z = 4$ μm) and 0.134 (for $z = 8$ μm). These values are comparable to, or slightly larger than, the predicted value (0.114) and the simulated value (0.121) for a flat surface. Nevertheless, cell contour variations and changes in focus may introduce additional variations in experimental measurements and contribute to cell-to-cell variations. For relative measurements of $g(0)$, this effect is likely to become less important and the average $g(0)$ value remains a reliable estimate of the mean number of aggregates per unit area. In contrast, $g(0) \cdot \bar{\imath}$, and the mean intensity is greatly underestimated since the out-of-focus membrane contributes less to the intensity (22).

The out-of-focus membrane experiences an effective beam size greater than that at the focus which broadens the fluctuation peaks and results in an increase in the estimate of w by a small amount. This may contribute to the systematically larger beam observed in S-FCS fits (0.86 μm) compared to the expected value (0.75).

Sensitivity to Aggregation

The limited statistical accuracy arising from the combination of short record lengths and cell heterogeneity raises the question of how sensitive the S-FCS experiments will be to changes in aggregation. Table II shows the results of simulations conducted with different extents of aggregation along with the corresponding predicted values of $g(0)$, $\bar{\imath}$, $g(0) \cdot \bar{\imath}$, and w. The predicted values are derived from the theoretical results of Table I and the input parameters. The simulated and predicted results correspond closely and are in all cases within the statistical accuracy of the experiment. These results suggest that the S-FCS experiment can be sensitive to fairly small changes in the aggregation distribution (e.g., from pentamers to decamers). The results in Table II also illustrate that the number of monomers per aggregate is correctly measured independently of the beam size (compare sets *A*1 and *A*2) and of the total surface density (compare sets *B* and *D*).

Table III-*A* shows $g(0)$ values measured on 3T3 cells labeled with FITC-S-conA at different concentrations when the cells were fixed before labeling to prevent lectin-induced cross-linking. There is no significant variation in $g(0)$ with concentration as expected for a partly aggregated receptor system: addition of more lectin increases the number of lectins bound per aggregate, but does not alter the number of aggregates per unit area as measured by the $g(0)$ value. Table III-*B* shows the changes

TABLE II
PREDICTED AND SIMULATED RESULTS FOR VARIOUS AGGREGATE DISTRIBUTIONS AND DENSITIES

Data Set	Density*	μ‡	$g(0)$	$\bar{\imath}$	$g(0)\cdot\bar{\imath}$	w
A1	1.67	1	0.175	2.45	0.425	0.93
predicted			0.191	2.62	0.500	1.00
A2	1.67	1	0.0448	9.51	0.436	1.77
predicted			0.0477	10.49	0.500	2.00
B	1.67	5	1.21	2.43	2.90	0.94
predicted			1.14	2.62	3.00	1.00
C	1.67	10	2.40	2.29	5.79	0.96
predicted			2.10	2.62	5.50	1.00
D	8.35	5	0.234	12.82	2.82	0.91
predicted			0.229	13.11	3.00	1.00

*density = number of particles per unit area.
‡μ = mean of unimodal Poisson aggregate distribution except for the monomer distribution for which $\sigma = 0$.

TABLE III
VARIATION IN $g(0)$ VALUES FOR FITC-S-conA ON 3T3 CELLS

A: cells fixed prior to lectin addition C_L^* μgmL^{-1}		$g(0) \pm$ SEM (N)
2.7		0.037 ± 0.018 (19)
8.0		0.065 ± 0.023 (24)
14.6		0.056 ± 0.014 (24)
25.3		0.045 ± 0.023 (24)
38.6		0.037 ± 0.013 (21)
66.5		0.080 ± 0.039 (24)
	Average	0.053 ± 0.017‡ (136)

B: cells fixed at time t after lectin addition t/min	$g(0) \pm$ SEM (N) (C_L = 9.4 μgmL^{-1})	$g(0) \pm$ SEM (N) (C_L = 47.2 μgmL^{-1})
3	—	0.080 ± 0.026 (21)
6	0.076 ± 0.035 (21)	0.140 ± 0.058 (15)
9	0.131 ± 0.053 (21)	0.123 ± 0.039 (14)
12	0.141 ± 0.080 (19)	0.151 ± 0.040 (41)
15	0.134 ± 0.071 (20)	0.205 ± 0.102 (13)

*FITC-S-ConA concentration.
‡standard deviation of average $g(0)$ values.

in $g(0)$ values resulting from lectin-induced cross-linking on cells that were exposed to FITC-S-conA before fixing. As the time of exposure increases, the $g(0)$ value increases, suggesting an increased level of aggregation. The 3–4-fold increase in $g(0)$ compared to Table III-*A* could be interpreted as an aggregation of mobile S-conA receptors by the lectin. Thus the mobile fraction (X_m) decreases and causes $g(0)$ to increase. In this system there is no independent assessment of the change in aggregation state. Nevertheless, these data illustrate that S-FCS measurements can detect fairly rapid changes in cell surface receptor distributions.

The lower limit of $g(0)$ values that can be measured reliably is not clear. On cell systems we have reproducibly measured $g(0)$ values as low as 0.005 corresponding to a particle density of $\sim 200/\mu m^2$. A series of measurements of ethidium bromide bound to DNA imbedded in polyacrylamide gels gave, for certain conditions, $g(0)$ values of ~0.002 corresponding to 500 particles per μm^2. Measurements on background, i.e. in solution or on areas of the coverslip where there is no labeling, typically gives $g(0)$ values ranging from 0.001 to 0.0001. Thus we feel the current upper limit on the particle density that can be estimated reliably is ~1,000 particles per μm^2. Experience with FPR experiments indicates that it is possible to measure 1,000 fluorophores per μm^2, particularly when long count times can be employed. The S-FCS experiments should therefore be capable of measuring monomeric distributions of receptors with density of ~1,000 monomers per μm^2, and since aggregation of these increases $g(0)$, it is also possible to study oligomers or polymers of the same receptors. Since many cells have surface areas of a few hundred μm^2, the S-FCS experiments should work for receptors with $\sim 10^5$ copies per cell. With larger surface densities the $g(0)$ value may become too small unless there is partial aggregation, while for lower surface densities the fluorescence detection is more difficult unless there are several fluorophores per receptor. The fundamental conclusion is that S-FCS measurements should work on systems that can be studied by FPR, and that monomer densities can be measured if they are below $\sim 10^3/\mu m^2$.

Karen L. Robinson provided valuable programming assistance, Peter T. Willard assisted in the simulation calculations as an NSERC Summer Undergraduate Scholar, Donata Frank and Thuy T. Pham contributed greatly to the experiments during their undergraduate research projects.

This work was supported by Natural Sciences and Engineering Research Council, Canada grant U-109.

Received for publication 19 April 1985 and in final form 6 September 1985.

REFERENCES

1. Webb, W. W., L. S. Barak, D. W. Tank, and E. -S. Wu. 1981. Molecular mobility on the cell surface. *Biochem. Soc. Symp.* 46:191–205.
2. Peters, R. 1981. Translational diffusion in the plasma membrane of single cells as studied by fluorescence microphotolysis. *Cell Biol. Int. Rep.* 5:733–760.
3. Petersen, N. O. 1984. Diffusion and aggregation in biological membranes. *Can. J. Biochem. Cell Biol.* 62:1158–1166.
4. Sheetz, M. P., M. Schindler, and D. E. Koppel. 1980. Lateral mobility of integral membrane proteins is increased in spherocytic erythrocytes. *Nature (Lond.).* 285:510–512.
5. Elson, E. L., and J. A. Reidler. 1979. Analysis of cell surface interactions by measurements of lateral mobility. *J. Supramol. Struct.* 12:481–489.
6. Shotton, D., K. Thompson, L. Wofsy, and D. Branton. 1978. Appearance and distribution of surface proteins of the human erythrocyte membrane. An electron microscope and immunochemical labelling study. *J. Cell Biol.* 76:512–531.
7. Roos, D. S., J. M. Robinson, and R. L. Davidson. 1983. Cell fusion and intramembranous particle distribution in polyethylene glycol resistant cells. *J. Cell Biol.* 97:909–918.
8. Schreiber, A. B., J. Hoebke, B. Vray, and A. D. Strosberg. 1980. Evidence for reversible microclustering of lentil lectin membrane receptors on HeLa cells. *FEBS (Fed. Eur. Biochem. Soc.) Lett.* 111:303–306.
9. Dale, R. E., J. Novros, S. Roth, M. Edidin, and L. Brand. 1981. Application of Forster long-range excitation energy transfer to the determination of distributions of fluorescently-labelled concanavalin A-receptor complexes at the surfaces of yeast and of normal and malignant fibroblasts. *In* Fluorescent Probes. G. S. Beddard and M. A. West, editors. Academic Press Inc., New York. pp. 159–181.
10. Schlessinger, J. 1980. The mechanism and role of hormone-induced clustering of membrane receptors. *Trends Biochem. Sci.* 5:210–214.
11. Cuatrecasas, P. 1983. Developing concepts in receptor research. *Drug Intell. Clin. Pharm.* 17:357–366.
12. Magde, D., W. W. Webb, and E. L. Elson. 1978. Fluorescence correlation spectroscopy. III. Uniform translation and laminar flow. *Biopolymers.* 17:361–376.
13. Weissman, M., H. Schindler, and G. Feher. 1976. Determination of molecular weights by fluctuation spectroscopy: application to DNA. *Proc. Natl. Acad. Sci. USA.* 73:2776–2780.

14. Peterson, N. O., D. C. Johnson, and M. J. Schlesinger. 1986. Scanning fluorescence correlation spectroscopy. II. Application to virus glycoprotein aggregation. *Biophys. J.* 49:817–820.
15. Elson, E. L., and W. W. Webb. 1975. Concentration correlation spectroscopy: a new biophysical probe based on occupation number fluctuations. *Annu. Rev. Biophys. Bioeng.* 4:311–334.
16. Weissman, M. B. 1981. Fluctuation spectroscopy. *Annu. Rev. Phys. Chem.* 32:205–232.
17. Elson, E. L., and D. Magde. 1974. Fluorescence correlation spectroscopy. I. Conceptual basis and theory. *Biopolymers.* 13:1–27.
18. Magde, D., E. L. Elson, and W. W. Webb. 1974. Fluorescence correlation spectroscopy. II. An experimental realization. *Biopolymers.* 13:29–61.
19. Petersen, N. O., S. Felder, and E. L. Elson. 1985. Measurement of lateral diffusion by fluorescence photobleaching recovery. *In* Handbook of Experimental Immunology. D. M. Weir, L. A. Herzenberg, C. C. Blackwell, and L. A. Herzenberg, editors. Blackwell Scientific Publications Ltd., Edinburgh. Chapter 24.
20. Petersen, N. O., and E. L. Elson. 1985. Measurements of diffusion and chemical kinetics by fluorescence photobleaching recovery and fluorescence correlation spectroscopy. *In* Methods in Enzymology. C. H. W. Hirs and S. N. Timasheff, editors. Academic Press Inc., New York.
21. Koppel, D. E., D. Axelrod, J. Schlessinger, E. L. Elson, and W. W. Webb. 1976. Dynamics of fluorescence marker concentration as a probe of mobility. *Biophys. J.* 16:1315–1329.
22. Petersen, N. O., and W. B. McConnaughey. 1981. Effects of multiple membranes on measurements of cell surface dynamics by fluorescence photobleaching. *J. Supramol. Struct. Cell. Biochem.* 17:213–221.
23. Koppel, D. E. 1974. Statistical accuracy in fluorescence correlation spectroscopy. *Phys. Rev.* A10:1938–1945.